KRUIF, C. G. DE (1976). Private communication, Utrecht.
KRUIF, C. G. DE & GINKEL VAN, C. H. D. (1977). *J. Chem. Thermodyn.* **9**, 725–730.
LEISEROWITZ, L. (1976*a*). *Acta Cryst.* B**32**, 775–802.
LEISEROWITZ, L. (1976*b*). Private communication.
LEISEROWITZ, L. & NADER, F. (1973). *Angew. Chem.* **85**, 150–151.
LIPPINCOTT, E. R. & SCHROEDER, R. (1955). *J. Chem. Phys.* **23**, 1099–1106.
LUCCHESI, C. A. & LEWIS, W. T. (1968). *J. Chem. Eng. Data*, **13**, 389–391.
MCGUIRE, R. F., MOMANY, F. A. & SCHERAGA, H. A. (1972). *J. Phys. Chem.* **76**, 375–393.
MARQUARDT, D. W. (1963). *SIAM (Soc. Ind. Appl. Math.) J. Appl. Math.* **11**, 431–441.
MATHEWS, D. M. & SHEETS, R. W. (1969). *J. Chem. Soc.* pp. 2203–2206.
MINICOZZI, W. P. & BRADLEY, D. F. (1969). *J. Comput. Phys.* **4**, 118–137.
MINICOZZI, W. P. & STROOT, M. T. (1970). *J. Comput. Phys.* **6**, 95–104.
MIRSKY, K. V. (1976). *Acta Cryst.* A**32**, 199–207.
MOMANY, F. A. (1976). *Environmental Effects on Molecular Structure and Properties*, edited by B. PULLMAN, pp. 437–458. Dordrecht, Holland: Reidel.
MOMANY, F. A., CARRUTHERS, L. M., MCGUIRE, R. F. & SCHERAGA, H. A. (1974). *J. Phys. Chem.* **78**, 1595–1620.
NAHRINGBAUER, I. (1970). *Acta Chem. Scand.* **24**, 453–462.
NAHRINGBAUER, I. (1975). Private communication.
SCHROEDER, R. & LIPPINCOTT, E. R. (1957). *J. Am. Chem. Soc.* **61**, 921–928.
SCHUSTER, P. (1976). *The Hydrogen Bond. I. Theory*, edited by P. SCHUSTER, G. ZUNDEL & C. SANDORFY, ch. 2, pp. 25–164. Amsterdam: North Holland.
SHIPMAN, L. L., BURGESS, A. W. & SCHERAGA, H. A. (1975). *Proc. Natl Acad. Sci. USA*, **72**, 543–547.
SIM, G. A., ROBERTSON, J. M. & GOODWIN, T. H. (1955). *Acta Cryst.* **8**, 157–164.
SKORCZYK, R. (1976). *Acta Cryst.* A**32**, 447–452.
SMIT, P. H., DERISSEN, J. L. & VAN DUIJNEVELDT, F. B. (1977). *J. Chem. Phys.* **67**, 274–282.
SMIT, P. H., DERISSEN, J. L. & VAN DUIJNEVELDT, F. B. (1978*a*). *Mol. Phys.* Submitted.
SMIT, P. H., DERISSEN, J. L. & VAN DUIJNEVELDT, F. B. (1978*b*). *Mol. Phys.* Submitted.
STRIETER, F. J., TEMPLETON, D. H., SCHEUERMAN, R. F. & SASS, R. L. (1962). *Acta. Cryst.* **15**, 1233–1239.
WARSHEL, A. & LIFSON, S. (1970). *J. Chem. Phys.* **53**, 582–594.
WILLIAMS, D. E. (1966). *J. Chem. Phys.* **45**, 3770–3778.
WILLIAMS, D. E. (1971). *Acta Cryst.* A**27**, 452–455.
WILLIAMS, D. E. (1974). *Acta Cryst.* A**30**, 71–77.

Acta Cryst. (1978). A**34**, 853–859

Aspects of Symmetry in Electron Diffraction Patterns and Optical Transforms of Very Small Homo-atomic Aggregates using Computer Simulation

BY P. LARROQUE AND M. BRIEU

Laboratoire de Physique Structurale, Université Paul Sabatier, 31077 *Toulouse CEDEX, France*

(*Received* 17 *October* 1977; *accepted* 28 *April* 1978)

This study investigates the reasons why it may happen that the first simulation of an electron diffraction pattern is not always centrosymmetrical whereas the second one is bound to be so. The formal link between the two simulations is established. A number of examples are given.

Introduction

Performance in selected-area electron diffraction is improving constantly. Twenty years ago resolution was about 2000 Å on a single grain; but quite recently an improved value of about 22 Å has been achieved by Geiss (1975) thanks to the latest progress in electron microscopes and the use of solid-state detectors.

Geiss's achievement, added to current interest in the problem of the structure of atom aggregates, and linked in particular with the study of nucleation, would seem to confirm the interest in the computer simulation of the diffraction patterns of such aggregates. This is, in fact, the subject of previous articles by the present authors (Larroque, Brieu & Lafourcade, 1976; Brieu, Larroque & Lafourcade, 1977) and here we would like to refer back to some aspects of these calculated patterns and in particular to the symmetries which are elicited.

Simulated electron diffraction pattern

If we assume u and v to be any two atoms of the aggregate, $\mathbf{r}_{uv}$ the interatomic vector of the pair uv and $\mathbf{S}$ the

scattering vector, for an incident electron beam of wavelength λ, given by $\mathbf{S} = (\mathbf{s} - \mathbf{s}_0)/\lambda$ (with the usual notation recalled in Fig. 5), then, in the homo-atomic example, the diffracted kinematical intensity I (Guinier, 1964) is given by

$$I = f^2 \sum_{u,v} \exp(j2\pi \mathbf{s} . \mathbf{r}_{uv})$$

(f: atom scattering factor for electrons). The function $I(\mathbf{S})$, related to the interatomic vectors of the aggregate, is described in reciprocal space and is centrosymmetrical (CS) in relation to the origin O of this space.

Given the fact that the investigator would normally tend to be influenced by the approximation, usually accepted as valid in electron diffraction, that the pattern on the photographic plate is a projection of the section of the reciprocal figure by a *plane* passing through O and perpendicular to $\mathbf{s}_0$, he would then be tempted to predict the centrosymmetry (CS) of the so-called pattern. We are going to show that this is not necessarily the case.

Figs. 1 to 4 show the simulations of the function I, *i.e.* selected-area diffraction pattern simulations, in some simple cases for $\lambda/a = 1/100$ (a: reference length corresponding to the lattice constant of the infinite crystal): a pair of atoms (Fig. 1), a regular tetrahedron (Fig. 2), a cuboctahedron of 13 atoms (Fig. 3), an icosahedron of 13 atoms (Fig. 4). The inset above each simulated pattern shows the orientation of the diffracting object with regard to the incident beam.

Fig. 1 corresponds to a borderline case which is easily forecast and included here only to illustrate the

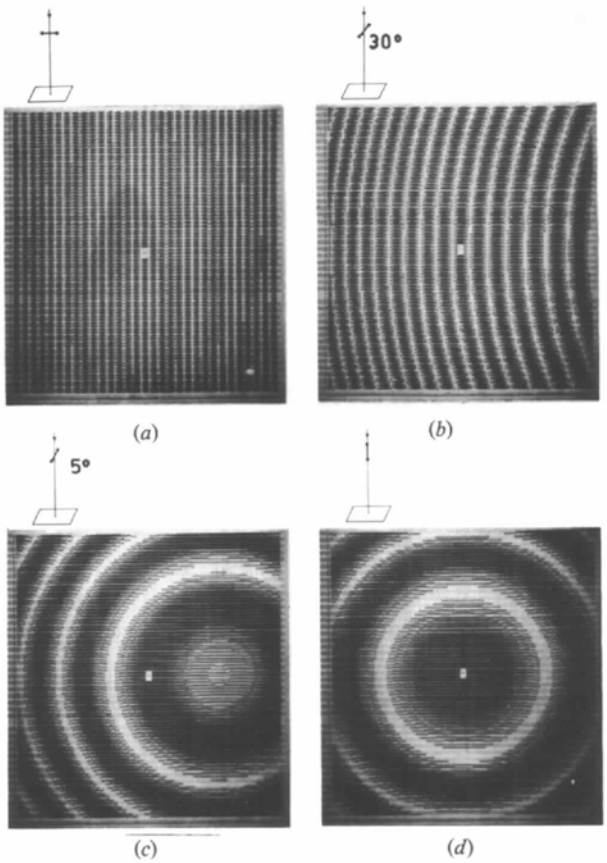

Fig. 1. Diffraction by a pair of atoms (for this figure, the step in scattering angle has been enlarged by three compared to the following ones and only the function I/f^2 has been drawn). (*a*) and (*d*) are the electronic analogues of Young's and Pohl's optical experiments, both of them being well known.

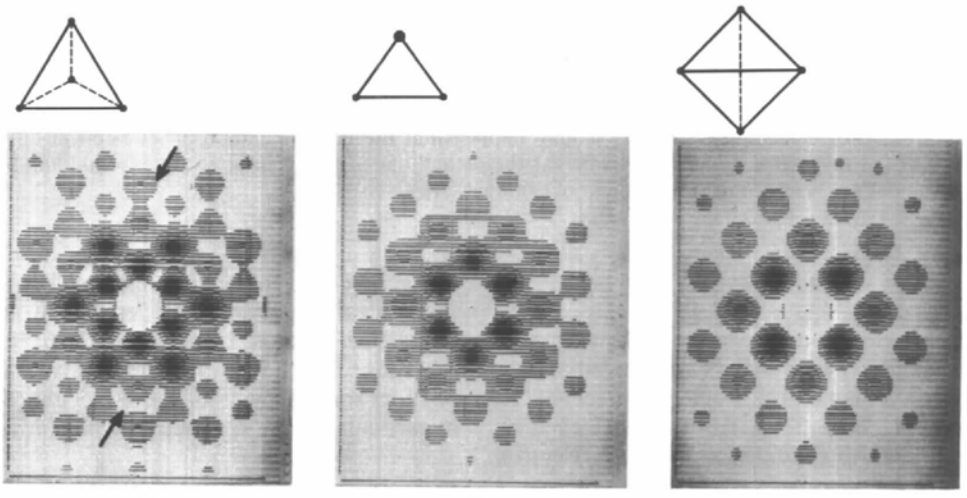

Fig. 2. Simulated diffraction pattern of four atoms associated in a regular tetrahedron. The CS is only obtained for cases (*b*) and (*c*) (for this simulation and the following, the f value for gold has been taken, and, in order to allow an improvement of contrast, the simulation of the central region has been deliberately avoided). The black arrows indicate some non-CS regions. The insets show a sketch of the aggregate when the incident beam is assumed perpendicular to the plane of the figure.

reliability of our calculations. The interpretation becomes evident when we consider the cones of interference which have the pair as an axis. The CS of Fig. 1(*a*) and (*d*), and the non-CS of Fig. 1(*b*) and (*c*) are easily deduced.

For Figs. 2 to 4, the legends specify the CS cases. The explanation of its presence or absence depends on Ewald's construction (Fig. 5), according to which, as a general rule, the cross section of the reciprocal figure is made by a *sphere*; it may result in $I_1 \neq I_2$, whereas $I_1 = I_3$ (I_1, I_2 and I_3 are the intensities calculated respectively at the points 1, 2 and 3 of Fig. 5). However, the gap between I_1 and I_2 remains small (it does not exceed 15% of the maximum intensity in our examples). This is because, with mean-energy electron diffraction, the gap between points 2 and 3 is also small (about a tenth of a thousandth of the radius of Ewald's sphere for a reflection close to the central spot). The effect observed in the long run, *i.e.* CS or non-CS pattern, is therefore noticeable only on weak 'secondary' reflections. However, for these reflections to be visible the population of the aggregate would need to be small, for example lower than a hundred atoms. This is what the examples dealt with in Fig. 6 reveal. In these examples one notices that, for an adapted structure and azimuth, a clearly deteriorated CS for the smallest of the aggregates is progressively restored as the size of the latter increases.

The influence of the curvature of the sphere may be brought to light by calculations carried out for different values of λ. One can see (Fig. 7) that the CS improves if one simulates an increase in the radius of the sphere,

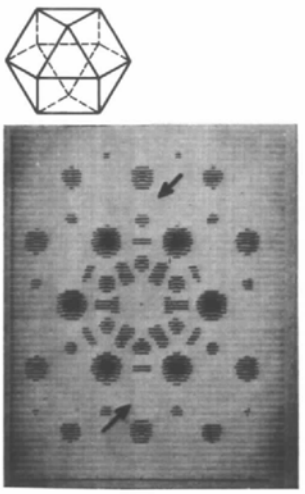

Fig. 3. Simulated diffraction pattern of a cuboctahedron of 13 atoms observed under the azimuth A_3. The pattern of this CS aggregate is not perfectly CS. The black arrows indicate some non-CS regions.

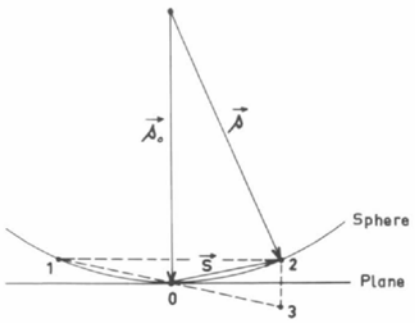

Fig. 5. A reminder of Ewald's construction.

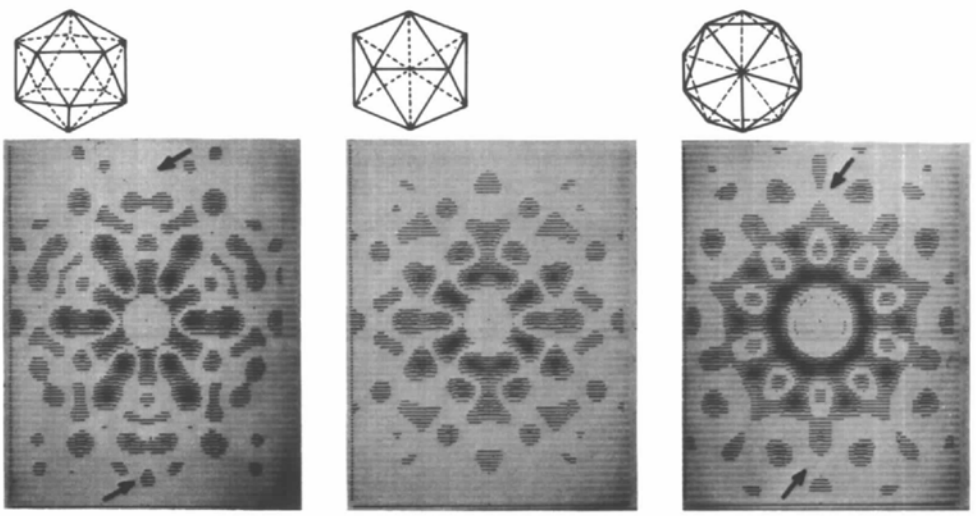

(*a*) (*b*) (*c*)

Fig. 4. Simulated diffraction pattern of an icosahedron of 13 atoms. The CS is obtained only in case (*b*). The black arrows indicate some non-CS regions.

that is to say a decrease in λ/a, or an increase in the accelerating voltage V.

As a conclusion to this study a simple rule which governs these problems of symmetry can be formulated as follows: every symmetry condition which aims to satisfy the equation $I_1 = I_2$ generates the CS of the pattern.

In other words, the diffraction pattern of an aggregate is CS if the latter has a symmetry plane perpendicular to the incident beam or a twofold symmetry axis parallel to the incident beam.

A geometrical analysis, shown in the Appendix, makes it possible to reproduce some of our former conclusions.

Simulated optical transform

The question may be asked why optical transform (Taylor & Lipson, 1964) does not raise the symmetry problem analysed above and why in fact it even makes the CS of the simulated pattern the test of the validity of the result obtained.

By means of calculation, we decided to simulate the approximation realized in an optical transform, *i.e.* the diffraction by the figure obtained when projecting the aggregate on a plane perpendicular to the incident beam (such a projection corresponds to the mask used in an optical diffractometer). This transformation associates each interatomic vector $\mathbf{r}_{uv}$ with its projection $\mathbf{r}_{uv\perp}$.

Formula (1) giving the diffracted intensity becomes for the new diffracting structure

$$I' = f^2 \sum_{u,v} \exp(j2\pi \mathbf{S} \cdot \mathbf{r}_{uv\perp}).$$

Or, by calling $\mathbf{S}_\perp$ the component of $\mathbf{S}$ perpendicular to the incident beam,

$$I' = f^2 \sum_{u,v} \exp(j2\pi \mathbf{S}_\perp \cdot \mathbf{r}_{uv\perp}). \qquad (2)$$

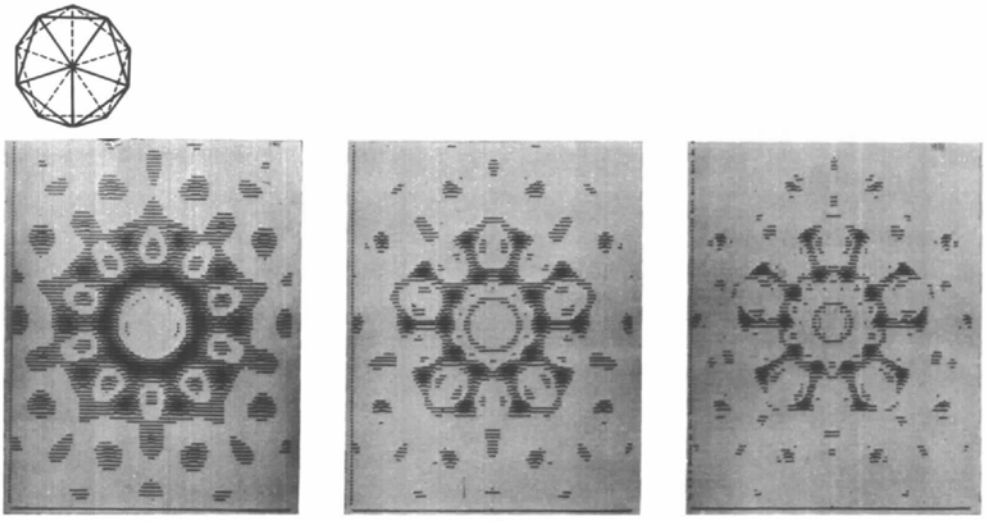

(*a*) (*b*) (*c*)

Fig. 6. Evolution of the CS of the simulated pattern for aggregates of the same icosahedral structure, observed under the same azimuth A_5, but of different sizes: (*a*) 13 atoms, (*b*) 55 atoms, (*c*) 147 atoms ($\lambda/a = 1/100$).

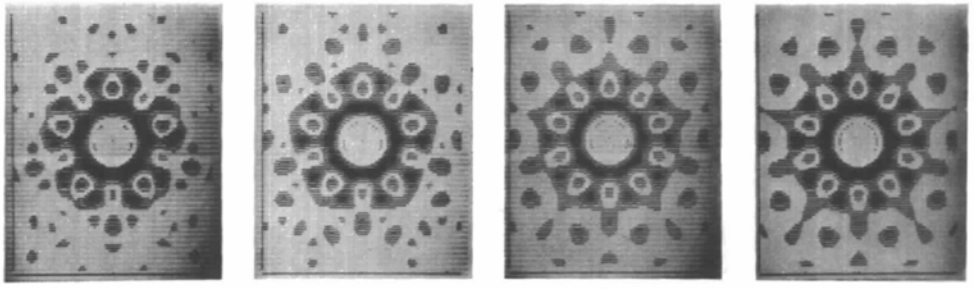

(*a*) (*b*) (*c*) (*d*)

Fig. 7. Evolution, as a function of the values of λ/a, of the symmetry of the simulated pattern, for an icosahedral aggregate of 13 atoms viewed under the azimuth A_5. The values of λ/a are (*a*) 4/100 ($V \simeq 5500$ V), (*b*) 2/100, (*c*) 1/100, (*d*) 1/200 ($V \simeq 250\,000$ V).

Relation (2) is simply the optical transform of the aggregate. It must then give, by computer simulation, a pattern identical to that obtained by optical simulation. This pattern is automatically CS, since it is the result of a planar central cross-section of the reciprocal figure of the aggregate projection.

To illustrate the relation (2) we have simulated the optical transform of the following models on a computer: hexagon (Fig. 8), tetrahedron (Fig. 9), cuboctahedron of 13 atoms (Fig. 10), icosahedron of 13 atoms (Fig. 11). Fig. 8 is identical to a previously published effective optical simulation (Taylor & Lipson, 1974), which substantiates our former analysis. Furthermore, all our calculated optical transforms are CS and, from this point of view, it is interesting to compare Figs. 9, 10 and 11 with the corresponding Figs. 2, 3 and 4.

Comparison between the two types of computer simulation

A more detailed comparison between the simulations in Figs. 2(*a*) and 9(*a*), 3 and 10, 4(*a*) and 11(*a*) suggests a further observation. In each case, the diffraction figure of a volumic aggregate is compared with that of a flat aggregate possessing the same number of atoms, with identical $\mathbf{r}_{uv\perp}$. One can see from the simulations the similar general aspect of these figures with, however, obvious differences in detail which must consequently be ascribed to the loss of the $\mathbf{r}_{uv\parallel}$ for flat aggregates ($\mathbf{r}_{uv\parallel}$ is the component of the interatomic vector $\mathbf{r}_{uv}$ parallel to the incident beam). Therefore, the general characteristics of the diffraction pattern are ruled by the $\mathbf{r}_{uv\perp}$. This conclusion is to be compared with that of Lafourcade (1954) according to which the angular width of the beam contributing to a diffraction spot is determined by the length of the atom rows in the diffracting crystallite which are normal to the beam.

A difficulty may appear during the calculation of the optical transform of a volumic aggregate. It may happen that, when projecting the structure, some atoms are projected on the same point. The loss of information resulting from the loss of the $\mathbf{r}_{uv\parallel}$ is then aggravated here by a phenomenon of overlapping: the projection includes fewer diffracting centres than the real aggregate. The result may be analysed in Fig. 11(*b*) and (*c*) which, supposedly simulating the diffraction by an

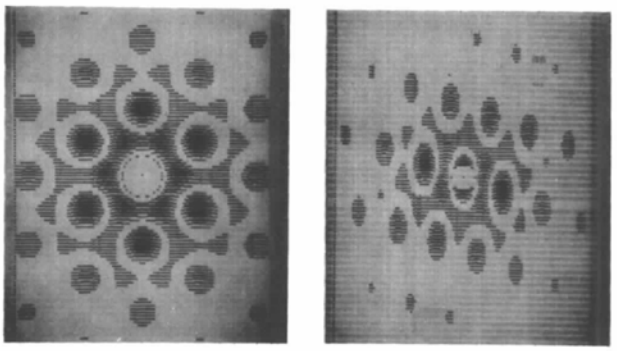

(*a*) (*b*)

Fig. 8. Computed optical transform of a hexagon (*a*) normal to the incident beam, (*b*) inclined with respect to the incident beam.

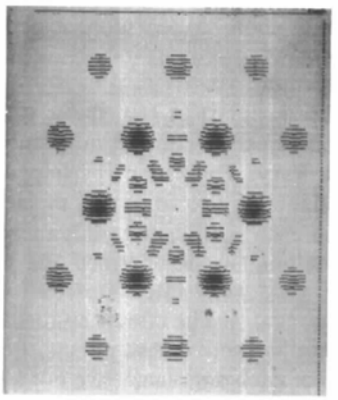

Fig. 10. Computed optical transform of a cuboctahedron of 13 atoms seen under the azimuth A_3. Compare with Fig. 3.

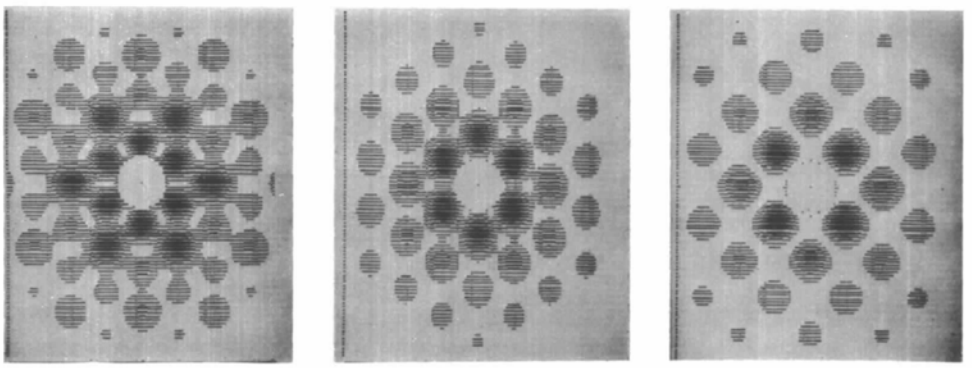

(*a*) (*b*) (*c*)

Fig. 9. Computed optical transform of a regular tetrahedron. Compare with Fig. 2.

icosahedron of 13 atoms, corresponds in fact to masks of 9 and 11 atoms only respectively. One can see that this loss may have an important effect on the diffraction figure leading, in extreme cases, to the inversion of some contrasts (Figs. 4*b* and 11*b*) or even to a complete modification of the said figure (Figs. 4*c* and 11*c*). With the 'pair of atoms' (Fig. 1), the computed patterns show the progressive transformation (Fig. 1*b* and *c*) of the straight parallel fringes of Fig. 1(*a*) into the rings of Fig. 1(*d*); the result would be quite different in optical transforms where straight parallel fringes would be found in the three cases of Fig. 1(*a*), (*b*) and (*c*).

These examples reveal a weak point of the optical transform which is also observed in effective optical simulation. The problem which consequently arises furthermore becomes insoluble when the superposition of two or several atoms of different nature takes place. In this case, the complete calculation of the diffraction pattern seems to give the only quantitative reference worth using.

Conclusion

The aspects of symmetry which we have considered in this article may soon have a more experimental basis when it becomes possible to produce and record electron diffraction patterns of aggregates having dimensions inferior to 15 Å (*i.e.* about 100 atoms), and when, of course, the interpretation of the patterns becomes necessary. This is not perhaps an unreasonable hope since the electro-optics of electron microscopes are already sufficiently advanced. The main problem remaining is to perfect the technique of recording the very weak intensities diffracted by such very small aggregates. The effects studied in this article could then be observed. These effects, inherent to the small volume of each aggregate, are not always easy to interpret using optical simulation by means of planar models. Our study might then contribute to the understanding of structural anomalies which occur at the first stages of the process of nucleation (Renou, Gillet, Brieu & Larroque, 1977).

APPENDIX

Some conditions for the CS of the diffraction pattern of an aggregate can be re-established by simple geometrical reasoning. Below we apply this kind of approach to the case of a homo-atomic aggregate.

We can classify the terms of the function I into three classes: (1) Those relevant to the $\mathbf{r}_{uv}$ perpendicular to the incident beam (Figs. 1*a*, 12*a* and 13*a*) contribute to the CS of the pattern. (2) Those relevant to the $\mathbf{r}_{uv}$ parallel to the incident beam (Figs. 1*d* and 12*b*), by their presence, imply a symmetry of revolution and therefore favour the CS. (3) Finally, those relative to the $\mathbf{r}_{uv}$ inclined to the incident beam have a less immediate effect. If only one pair uv is present, Figs. 1(*b*), 1(*c*) and 12(*c*) show that its contribution is non-CS.

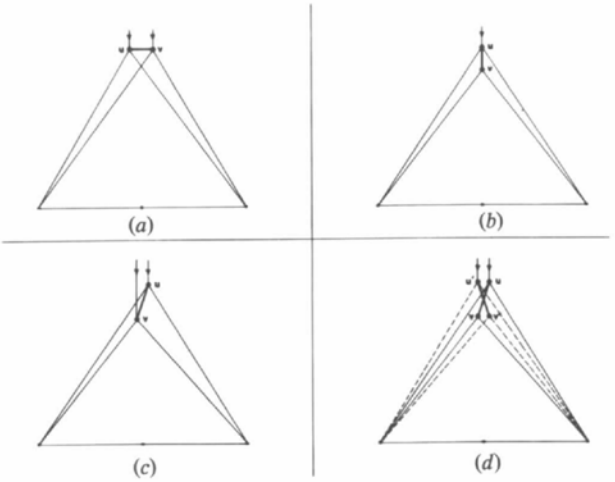

Fig. 12. Analysis of the contribution of the different pairs of atoms to the diffracted intensity.

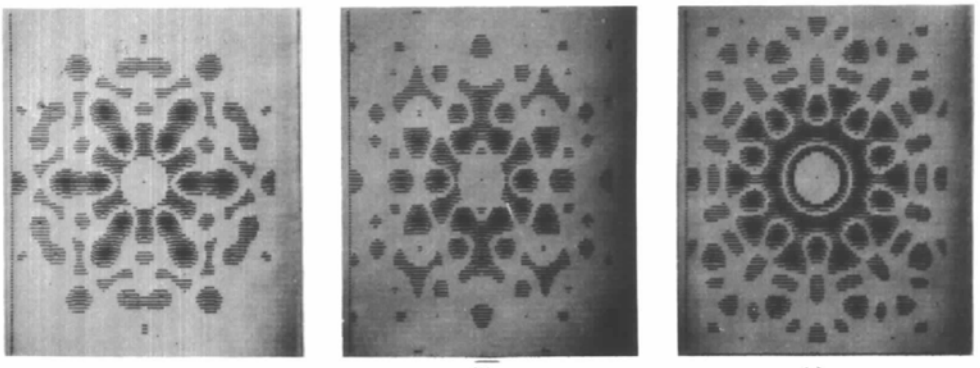

Fig. 11. Computed optical transform of an icosahedron of 13 atoms. Compare with Fig. 4.

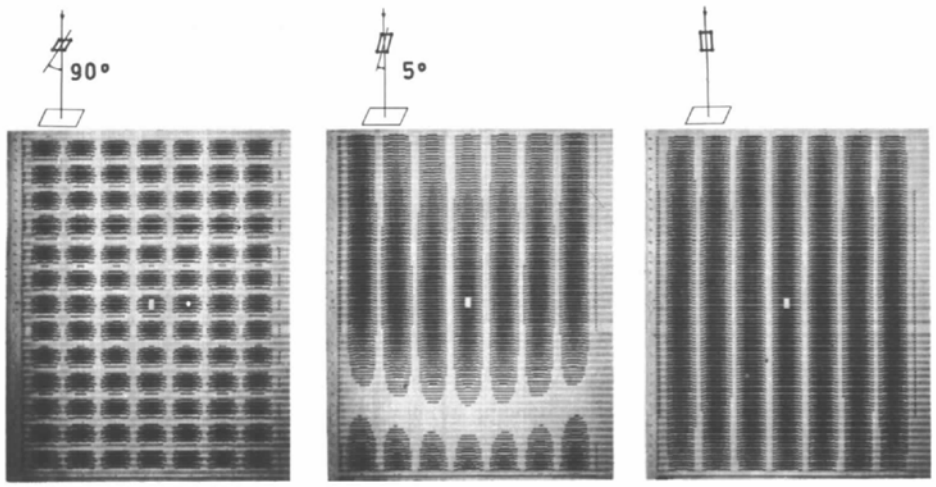

(*a*) (*b*) (*c*)

Fig. 13. Simulated diffraction pattern of a planar rectangular aggregate of four atoms. It may be noticed that the patterns (*b*) and (*c*) may be compared to reflection high-energy electron diffraction (RHEED) patterns.

In order to carry the discussion further, we need to develop the meaning of function I, by introducing after Vainshtein (1966) the notion of 'interatomic-distance function'. This analysis shows that each term of I acts as if the corresponding double pair uv, vu had been translated up to a hypothetical point where the middle or the origin of the interatomic vectors is finally superimposed. This is a consequence of the fact that only the components of the interatomic vectors intervene in the process. Let us consider a second pair $u'v'$, in such a way that, after the translation, the 'quadruplet' of the four inclined interatomic vectors uv, vu, $u'v'$, $v'u'$ has the particular configuration and position of Fig. 12(*d*), that is to say admits the incident beam as a symmetry axis. The result is the restoration of the CS (Fig. 13*c*). In Fig. 13(*b*) it may be verified that a 'quadruplet' having a different position with regard to the incident beam gives a non-CS pattern.

When we try to forecast the symmetry of the pattern of an aggregate, two cases are possible. (1) All the inclined $\mathbf{r}_{uv}$ are, after the translation, associable in 'quadruplets' in an appropriate position (Fig. 12*d*): the pattern is perfectly CS.

(2) Some oblique $\mathbf{r}_{uv}$ escape this grouping (for instance those which are binding atoms on the periphery of the aggregate): the pattern is then not thoroughly CS.

When the initial nucleus evolves and develops into a crystal, the symmetry of the infinite structure appears progressively. From now on, when the azimuth of the incident beam is taken into account, if a quadruplet is in the appropriate position to the CS, the probability of several of them existing in the same position increases at the same time. The CS then becomes more and more evident by decreasing, in relative value, the disturbing effect eventually produced by the non-associable pairs or the quadruplets in an inappropriate position.

This reasoning is obviously less complete than that based on Ewald's construction. Although it enables us to link the CS to the structure and to the size of the aggregate as well as to the azimuth of observation, it does not allow us to foresee the evolution of the pattern as a function of wavelength. Finally, it may be pointed out that its use would become rather arduous if the population of the aggregate exceeded about ten atoms.

References

BRIEU, M., LARROQUE, P. & LAFOURCADE, L. (1977). *C. R. Acad. Sci. Sér. B*, **284**, 189–192.

GEISS, R. H. (1975). *Appl. Phys. Lett.* **27**, 174–176.

GUINIER, A. (1964). *Théorie et Technique de la Radiocristallographie*, 3rd ed., p. 408. Paris: Dunod.

LAFOURCADE, L. (1954). Thesis, Univ. de Toulouse.

LARROQUE, P., BRIEU, M. & LAFOURCADE, L. (1976). *C. R. Acad. Sci. Sér. B*, **282**, 309–312.

RENOU, A., GILLET, M., BRIEU, M. & LARROQUE, P. (1977). *Thin Solid Films*, **44**, 75–82.

TAYLOR, C. A. & LIPSON, H. (1964). *Optical Transforms*, 1st ed. London: Bell.

VAINSHTEIN, B. K. (1966). *Diffraction of X-rays by Chain Molecules*, Engl. trans., p. 29. Amsterdam: Elsevier.